https://doi.org/10.5194/acp-2022-628
Preprint. Discussion started: 23 September 2022


Atmospheric Chemistry and Physics Discussions

# Insoluble lipid film mediates the transfer of soluble saccharides from the sea to the atmosphere: the role of hydrogen bonding

Minglan Xu, Narcisse Tsona Tchinda, Jianlong Li, Lin Du*

Environment Research Institute, Shandong University, Binhai Road 72, Qingdao, 266237, China

Correspondence: Lin Du (lindu@sdu.edu.cn)

https://doi.org/10.5194/acp-2022-628
Preprint. Discussion started: 23 September 2022


Atmospheric Chemistry and Physics Discussions


## Abstract

Saccharides are a large group of organic matter in sea spray aerosol (SSA). Although they can affect climate-related properties of SSA, the mechanism through which saccharides are transferred from bulk seawater to the ocean surface and ultimately into SSA is still debated. Here, the transfer of small soluble saccharides was validated and quantified using a controlled plunging jet sea spray aerosol generator to better understand the wide range of particle properties produced by natural seawater mixed with model organic species, glucose and trehalose. Data show that both soluble saccharides can promote the production of SSA particles. Conversely, the role of the insoluble fatty acid film on the surface greatly reduced the production of SSA. The resulting inorganic-organic mixed particles identified by the transmission electron microscope (TEM) showed typical core-shell morphology. Langmuir model was used to parameterize the adsorption and distribution of saccharide into SSA across the bubble surface, while infrared reflection-absorption spectroscopy (IRRAS) combined with Langmuir isotherms were undertaken to examine the effects of aqueous subphase soluble saccharides on the phase behavior, structure and ordering of insoluble lipid monolayers absorbed at the air/water interface. Changes in alkyl chains and headgroups structure of mixed fatty acid monolayers under different saccharide concentrations in aqueous phase were reported. In seawater solution, the effects of dissolved saccharides on the ordering and organization of fatty acid chains were muted. Hydrogen bond analysis implied that soluble saccharide molecules displaced a large amount of water near the fatty acid polar headgroups. Saccharide-lipid interactions increased with

https://doi.org/10.5194/acp-2022-628
Preprint. Discussion started: 23 September 2022


Atmospheric Chemistry and Physics Discussions

increasing complexity of the saccharide in the order glucose < trehalose. Our results indicate that the interaction between soluble saccharides and insoluble fatty acid molecules through hydrogen bonds is an important component of the sea-air transfer mechanism of saccharides.

## 1 Introduction

Sea spray aerosol (SSA) represents the major source of aerosol particle populations and significantly impacts the earth's radiation budget, cloud formation and microphysics by serving as cloud condensation nuclei (CCN) and ice nuclei (IN), and microbial cycling (Bertram et al., 2018; Partanen et al., 2014). The formation of SSA particles is strongly influenced by the uppermost sea surface microlayer (SML), which is a thin layer of 1–1000 μm thickness formed due to different physicochemical properties of air and seawater (Wurl et al., 2017). Beyond sea salt, the ocean surface contains a fair amount of organic matter (OM) mass fraction, covering carbohydrates, lipids, proteins, humic-like, intact phytoplankton cells and fragments, fungi, viruses, and bacteria (Van Pinxteren et al., 2020; Cunliffe et al., 2013). The SML is involved in the generation of SSA, including their organic fractions by transferring OM to rising bubbles before they burst into film drops and jet drops (Wang et al., 2017). When a bubble reaches the water surface, destroying the surface membrane of the water, the bubble bursts into many so-called film droplets. After the bubble film breaks, a jet of water rising vertically from the ruptured bubble cavity forms so-called jet droplets. During this process, the film drops (<1 μm) leading to the formation of submicron

https://doi.org/10.5194/acp-2022-628
Preprint. Discussion started: 23 September 2022


Atmospheric Chemistry and Physics Discussions

particles are mainly OM-enriched compared to the larger jet drops (1–25 μm). Specific organics, such as surface-active OM, are highly enriched in SML relative to bulk seawater and contribute to surface film formation. They are mainly composed of phospholipids, fatty acids, fatty alcohols, sterols and more complex colloids and aggregates (Crocker et al., 2022; Van Pinxteren et al., 2022). Among these organics, the saturated fatty acids are the dominant contributors (Cochran et al., 2016). The chemical composition of SSA also depends on the physical properties of the breaking waves, which determines the distribution of OM at the air-sea interface and how it is transported from the SML into aerosol particles (Collins et al., 2014).

Surface-active biomolecules are preferentially transferred from marine surface water into the atmosphere through the bubble bursting processes, forming a considerable fraction of primary marine organic aerosols (Schmitt-Kopplin et al., 2012). Previous measurements have shown that up to 60% of ocean particle mass can be organic (with even a higher proportion for submicron particles), which exhibits a strong size dependence(O'dowd et al., 2004; Russell et al., 2010). Spectroscopic evidence from field-collected SSA particles indicates that the oxygen-rich organic fractions of individual particles contains molecular signatures of saccharides and carboxylic acids (Hawkins and Russell, 2010). For example, it has previously been observed that the carbohydrate-like spectroscopic signatures account for 40–61% of the submicron SSA organic mass (Quinn et al., 2014; Russell et al., 2010). A large portion of this mass is attributed to saccharides that are transferred from seawater to SSA, and shows a certain enrichment in SSA. Specifically, the high enrichment factor of carbohydrates was

https://doi.org/10.5194/acp-2022-628
Preprint. Discussion started: 23 September 2022


Atmospheric Chemistry and Physics Discussions

calculated for supermicron (20–4000) and submicron (40–167000) particles relative to the bulk seawater in the Western Antarctic Peninsula (Zeppenfeld et al., 2021). According to previous laboratory studies, marine bacteria, divalent cations and protein can affect the saccharide enrichment in SSA (Hasenecz et al., 2020; Schill et al., 2018). However, a mechanistic and predictable understanding of these complex and interacting processes in favor of saccharides found in marine aerosol particles remains largely unexplored, despite their oceanic and atmospheric significance. More fundamentally, the nature of marine organic aerosol particles composed of carbohydrates content and their ability to act as CCN or IN are not entirely disentangled (Orellana et al., 2011; Cochran et al., 2017; Wolf et al., 2019).

A variety of saccharides have been found ubiquitous in the ocean, including dissolved free monosaccharides, oligo/polysaccharides, sugar alcohols, and monosaccharide dehydrates, the composition of which depends on marine biological activity (Van Pinxteren et al., 2012). Frossard et al. (2014) used the hydroxyl characteristic functional group of atmospheric marine aerosols from Fourier transform infrared spectroscopy to infer the contributions of different saccharides in SSA. It was found that the primary marine aerosols produced in biologically productive seawater had stronger hydroxyl group absorption peak characteristic of monosaccharides and disaccharides, while the hydroxyl groups of seawater organic matter were closer to those of polysaccharides. This suggests that larger saccharides may be preferentially retained in seawater during aerosol production. Analysis of aerosol samples collected on the Western Antarctic Peninsula also showed that not only polysaccharides but also a high portion of free

https://doi.org/10.5194/acp-2022-628
Preprint. Discussion started: 23 September 2022


Atmospheric Chemistry and Physics Discussions

monosaccharides mainly composed of glucose, fructose, rhamnose and glucosamine were present (Zeppenfeld et al., 2021). Raman spectroscopy was used to measure individual SSA particles generated via wave breaking in a wave flume under algal bloom conditions to get a deeper insight into their organic categories. It was reported that 4%–17% and 3%–46% of sub- and supermicron particles show strong spectral characteristics of free saccharides and short-chain fatty acids, respectively (Cochran et al., 2017). However, current climate models largely underestimate the ratio of saccharides in marine aerosols (Cravigan et al., 2020). It is urgent to clarify the physicochemical mechanisms that drive free saccharides transfer to SSA.

A possible explanation for the SSA composition in saccharides involves the affinity between soluble saccharides and insoluble surfactant monolayers already adsorbed on the water surface, resulting in co-adsorption of the soluble saccharides (Link et al., 2019b). This co-adsorption arises from non-covalent interactions and promotes the binding of soluble organic matter to the surface with the headgroups of insoluble Langmuir film. Previous studies have indicated that the presence of lipids or proteins strongly enhances the surface adsorption capacity of saccharides, even for highly soluble saccharides that do not adsorb individually at the air/water interface (Pavinatto et al., 2007; Burrows et al., 2016). For example, recent studies have shown that simple, soluble biomolecules such as phenylalanine and trehalose exhibit an affinity for lipid films, altering membrane permeability and phase behavior (Perkins and Vaida, 2017; Link et al., 2019a). A divalent cation-mediated co-adsorption mechanism was also proposed to explain the enrichment of monosaccharide in laboratory-generated SSA

https://doi.org/10.5194/acp-2022-628
Preprint. Discussion started: 23 September 2022


Atmospheric Chemistry and Physics Discussions

(Schill et al., 2018). Alternatively, saccharides can be bound covalently to larger, more surface-active biomolecules, such as glycoproteins or lipopolysaccharides, which attach to SML and are eventually transferred into SSA through bubble bursting at the ocean surface (Estillore et al., 2017). Although different hypotheses have been proposed, there is still debate about the more nuanced mechanisms that guide the sugar-lipid interactions in the marine environment.

The present work aims to use a multipronged approach that combines bulk SSA production experiments, Langmuir surface pressure-area isotherms and infrared reflection-absorption spectroscopy (IRRAS) to examine the role of saccharides in SSA production and the mechanism of saccharides transfer and enrichment from aqueous solution into SSA. The study focuses on two small soluble saccharides that are prevalent in seawater, glucose and trehalose, which are uncharged monosaccharide and disaccharide, respectively. A plunging jet sea spray aerosol generator was used to generate nascent SSA particles by artificially generating bubbles in seawater as a mean of simulating sea spray production by breaking waves. This simulation helps evaluate the impact of soluble saccharides as well as fatty acids on SSA production and particle morphology. Langmuir isotherms provided abundant information for stability and fluidity of monolayers, which were used to adequately describe the magnitude of interaction effects between subphase soluble saccharides and surface insoluble surfactants. Finally, IRRAS spectra provided molecular scale descriptions of monolayer conformational information and allowed us to deduce the distribution of saccharide species at the interface. By combining all the data, we propose a model of sea-air

https://doi.org/10.5194/acp-2022-628
Preprint. Discussion started: 23 September 2022


Atmospheric Chemistry and Physics Discussions

transfer of marine saccharides through hydrogen bond interactions involved in surface insoluble lipid molecules.

## 2 Experimental section

### 2.1 Materials and solutions

D-(+)-Glucose (Glu, powder, ≥99.5%) and D-(+)-Trehalose anhydrous (Tre, powder, 99%) were purchased from Aladdin. Stearic acid (SA, >98%, TCI), palmitic acid (PA, >98%, Adamas-beta) and myristic acid (MA, ≥99.5%, Aladdin) were prepared in chloroform (AR, ≥99.0%, Sinopharm Chemical Reagent Co., Ltd) at a final concentration of 1 mM each. Figure S1 shows the chemical structures of the three fatty acids used in this study. The respective fatty acid solutions were mixed at a molar ratio of 2 MA:4 PA:3 SA to obtain a mixed lipid stock solution. All chemicals were used without further purification. The natural seawater (SW) was collected from Shazikou, Qingdao, China. Here, surface seawater was obtained from a pier on the coast by dipping high-density polyethylene containers trough the seawater surface. The sampled seawater was microfiltered through 0.2 μm polyethersulfone filter (Supor®-200, Pall Life Sciences, USA) to remove large particles such as sediments, algae and bacteria. The filtered seawater was used for SSA generation and as a filling subphase for interfacial experiments. Different concentrations of saccharide-containing seawater solution required in the experiments were obtained by dissolving different masses of glucose or trehalose in the filtered natural seawater using mechanical stirring.

https://doi.org/10.5194/acp-2022-628
Preprint. Discussion started: 23 September 2022


Atmospheric Chemistry and Physics Discussions

159 **2.2 SSA production and collection**

160 SSAs were produced using a plunging jet-sea spray aerosol generator (Figure 1). A
161 physical drawing of the aerosol generation system can be found in Figure S2. The
162 generator and its detailed operation principle has been described elsewhere (Liu et al.,
163 2022). Briefly, the generator consists of a stainless steel (shipboard class, 316L)
164 rectangular sealed container and a viewable glass window. The upper removable lid has
165 ports for water inlet, purging air, and sampling. The purge air is supplied by a zero-air
166 generator (Model 111, Thermo Scientific, USA) and the flow rate is controlled at 10 L
167 $min^{-1}$. A peristaltic pump (WL600-1A, ShenChen) periodically circulates water from
168 the bottom of the generator to the top nozzle through a Teflon tube with a pump speed
169 of 1 L $min^{-1}$, creating a plunging water column that hits the seawater surface and
170 entrains air into the bulk seawater. The bubble plumes extend approximately 15 cm
171 down into the water, a moderate depth considering that the majority of the air being
172 entrained in is located within about 50 cm from the sea surface (Hultin et al., 2010).
173 When the bubbles rise to the air/water interface and burst, they generate SSA emissions.
174 When studying insoluble surfactant effects, a concentrated solution of 1 mM mixed
175 fatty acids in chloroform was added to the surface of the seawater solution. After the
176 necessary fatty acids were added, only the sheath air flowed, allowing the chloroform
177 to evaporate for 15 min and leaving only the surfactant on the surface. After pre-
178 preparation for 15 min, the sheath air and peristaltic pump were turned on to produce
179 SSAs. Prior to collection, SSAs were dried to a relative humidity of ~40% using a
180 diffusion dryer. Thereafter, a scanning mobility particle sizer (SMPS, model 3936, TSI)

https://doi.org/10.5194/acp-2022-628
Preprint. Discussion started: 23 September 2022


Atmospheric Chemistry and Physics Discussions

consisting of a differential mobility analyzer (DMA, model 3081, TSI Inc., USA) and a condensation particle counter (CPC, model 3776, TSI Inc., USA) was used to measure the particle size distributions and number concentrations, respectively. The particle size distribution ranging from 13.6 to 710.5 nm was obtained at a sheath flow rate of 3.0 L $min^{-1}$ and aerosol flow rate of 0.3 L $min^{-1}$. Dried SSAs were deposited onto 200 mesh copper grids with carbon foil (T11023, Tilan, China) by a single particle sampler (DKL-2, Genstar electronic technology Co., Ltd) to further characterize the particle morphology.

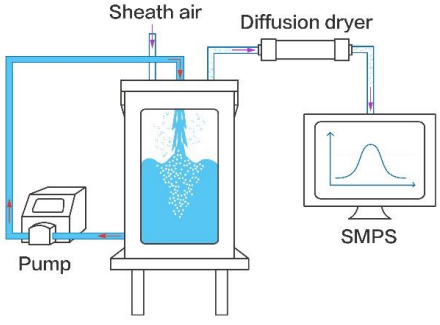


Figure 1. Schematic picture of the plunging jet-sea spray aerosol generator. The red arrows represent the flow direction of seawater, and the purple arrows represent the flow of gases and aerosols.

### 2.3 Langmuir monolayer preparation and Langmuir isotherms

The Langmuir trough setup has been described previously (Xu et al., 2021). Briefly, it consists of a rectangular Teflon trough (Riegler & Kirstein, Germany) and two moveable Teflon barriers whose movements are precisely controlled to achieve

https://doi.org/10.5194/acp-2022-628
Preprint. Discussion started: 23 September 2022


Atmospheric Chemistry and Physics Discussions

symmetric compression of the monolayer at the air/water interface. A Wilhelmy plate attached to the pressure sensor was used to measure the surface pressure. Each 100 mL subphase consisted of natural seawater, with varying amounts of glucose or trehalose. Aliquots of mixed fatty acids stock solution were spread onto the subphase surface dropwise with a glass microsyringe and 15–20 min were allowed for solvent evaporation. The surface pressure ($\pi$), given by eq 1 and defined as the difference in surface tension between the pure air/water interface ($\gamma_0$) and the monolayer covered interface ($\gamma$) was monitored.

$$\pi=\gamma_0-\gamma \quad (1)$$

The barriers were compressed at 3 mm $min^{-1}$ and isotherm data were collected for surface pressure $\pi$ (mN $m^{-1}$) versus area per molecule ($Å^2$). All experiments were performed at (22 ± 3) ℃ and relative humidity below 65%.

### 2.4 Infrared reflection-absorption spectroscopy measurement

The polarization-modulation infrared reflection-absorption spectroscopy (PM-IRRAS) is a mainstream spectroscopic method for in-situ characterization of Langmuir monolayers at the molecular level. For IRRAS spectra, floating monolayers were spread at the aqueous subphase and compressed to the desired surface pressure, and stopped before obtaining the spectra. PM-IRRAS spectra were obtained using a Fourier transform infrared (FT-IR) spectrometer (Bruker Vertex 70, Germany) equipped with an external reflection accessory (XA-511). The interference infrared beam was set out from FT-IR and polarized by a ZnSe polarizer to alternately generate s- and p-

https://doi.org/10.5194/acp-2022-628
Preprint. Discussion started: 23 September 2022


Atmospheric Chemistry and Physics Discussions

polarization lights. They were then continuously modulated by a photoelastic modulator (PEM-100) at a high frequency of 42 kHz to measure the spectra of both polarizations simultaneously. The infrared beam was focused onto the Langmuir film through a gold mirror, and then a portion of reflected light was directed onto the liquid nitrogen-cooled mercury-cadmium-telluride (MCT) detector. The application of polarization modulation attenuates the noise of reflective FT-IR and the interference of water vapor and carbon dioxide. The spectra given here are Reflectance-Absorbance (*RA*) given as:

$$RA = -\log(R/R_0) \quad (2)$$

where $R$ and $R_0$ are the reflectance of fatty acid solution and pure water, respectively. To obtain a better signal-to-noise ratio, spectra were collected with 2000 scans and 8 $cm^{-1}$ resolution at a fixed incidence angle of 40°. Data analysis was processed using OPUS software for each displayed spectrum.

### 2.5 Transmission electron microscope imaging

Particle imaging was performed using a transmission electron microscope (TEM, FEI Tecnai G2 F20, FEI, USA) equipped with a Schottky field emission gun. It was operated at an accelerated voltage of 20–200 kV with a high angle annular dark field detector to collect TEM images and even preserve the soft internal structure of organic sources under high vacuum conditions.

https://doi.org/10.5194/acp-2022-628
Preprint. Discussion started: 23 September 2022


Atmospheric Chemistry and Physics Discussions

## 3 Results and discussion

### 3.1 SSA particle number size distributions

To test the transfer of soluble saccharides and their interaction with insoluble fatty acids, experiments were carried out with seawater containing 1.0 g $L^{-1}$ glucose or trehalose, and particle number size distributions were obtained for each set of experiments. Figure 2 shows the particle number size distributions resulting from seawater to which different soluble saccharides were added in the presence or absence of fatty acids on the surface. As a reference, the particle size distribution produced from natural seawater is also given. The submicron particle size distributions produced by the plunging jet generator are well represented by lognormal mode. In the absence of saccharide, a broad, unimodal distribution of SSA with a peak number concentration around 168 nm was generated. This observation agrees quite well with previous studies that produced SSA by the plunging jet method (Christiansen et al., 2019; Prather et al., 2013). Moreover, the SSA yielded by plunging jet also has a size distribution similar to that yielded by the breaking wave, which particle number size distribution is ~162 nm. This contrasts with most previous laboratory studies using sintered glass filters or frits, which tend to exhibit a smaller mean diameter and narrower distribution. This may be because similar bubble size distributions exist in the two generation mechanisms using plunging jets and breaking waves. More notably, a marine accumulation mode with particle diameter of 170 nm (geometric mean diameter, 30% RH) was also employed in the widely used GEOS-Chem model based on the measurements of Quinn et al (Jaegle et al., 2011).

https://doi.org/10.5194/acp-2022-628
Preprint. Discussion started: 23 September 2022


Atmospheric Chemistry and Physics Discussions

Laboratory studies of the effects of saccharide organic substances on droplet production have been inconclusive. A previous study has used two bubble generation methods (plunging water jet and diffusion aeration) to investigate the number size distribution of SSA particles produced by mixing fructose and mannose with NaCl or artificial seawater solution (King et al., 2012). The results showed that the yield of SSA particles containing sodium dodecyl sulfate was significantly lower than that containing fructose, but the yield of SSA particles containing mannose was lower than that containing sodium laurate. Lv et al. (2020) found that addition fructose to sea salt solution can significantly promote the increase of SSA number concentration. However, the above studies lacked direct comparative results on SSA production influenced by different soluble saccharides. For the plunging jet, our measurements indicate that soluble saccharides can promote the production of SSA to varying degrees. It was observed that glucose led to a slight increase in particle number concentration, increasing the diameters to ~175 nm. As a contrast, the natural seawater spiked with trehalose resulted in a higher total particle number concentration over a wide size range. Therefore, the change in production and properties of SSA from actual seawater may be more complicated under the influence of different saccharides.

https://doi.org/10.5194/acp-2022-628
Preprint. Discussion started: 23 September 2022


Atmospheric Chemistry and Physics Discussions

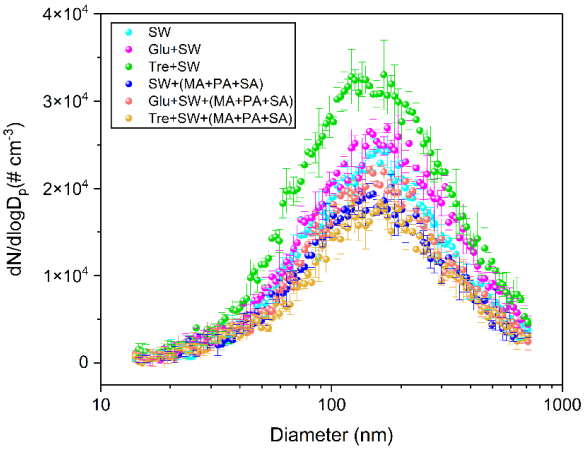


Figure 2. The particle number size distribution spectra of SSAs produced from blank seawater sample and seawater sample spiked with glucose or trehalose. Both results are presented here with and without fatty acid surface films.

The effect of the interaction of insoluble fatty acids with different saccharides on SSA particles was investigated by spreading insoluble fatty acids on seawater surface. In plain sight, fatty acids on the surface can significantly reduce the number concentration of SSA regardless of the presence of saccharides in the seawater. Moreover, fatty acids show the highest inhibitory effect on SSA produced by trehalose-containing seawater solution. There are at least two mechanisms by which soluble saccharides may affect particle production. On the first hand, it may stabilize or destabilize bubbles on the water surface by associating with other substances favoring co-aerosolization processes. On the other hand, soluble saccharides may influence bubble bursting through changes in water and bubble surface tension. We ascribe that the surface layer is significantly more stable, resulting in less bubble bursting in the fatty acids case than in the glucose and trehalose case. Collectively, the observed

https://doi.org/10.5194/acp-2022-628
Preprint. Discussion started: 23 September 2022


Atmospheric Chemistry and Physics Discussions

variability in these experiments suggests an urgent need to better build the link between total SSA particle flux and seawater organic composition over the ocean. However, sole bulk-phase generation experiments may not accurately capture the relevant chemical behaviors and support mechanism analysis that occur in the SML. Therefore, we attempted to explore the possible interaction mechanisms via air/water interface chemical experiments.

### 3.2 π-A isotherms of fatty acid monolayer

In this section, we only discuss traditional Langmuir monolayers, which operate on air/water interfaces that are ubiquitous along the sea surface (Elliott et al., 2014). The π-A isotherm reflects information on the phase behavior of the monolayer as a function of lipid packing density. As shown in Figure 3, the π-A isotherms of individual and mixed fatty acids on the natural seawater subphase are presented. When the mechanical barriers initially begin to compress, the amphiphilic molecules in the monolayer are in the gaseous (G) phase under a large area per molecule, with the hydrophobic tails having significant contact with the water surface, but little contact with each other. At this stage, the compression of the film does not lead to a significant change in surface pressure. As the monolayer is compressed, the intermolecular distances gradually decrease and the surface pressure begins to rise from zero into the liquid expanded (LE) phase, where the hydrophobic tails start to touch each other, but remain largely disordered and fluid. This is represented as the lift-off area of the isotherm. Further compression results in a thermodynamic transition to a liquid condensed (LC) phase.

https://doi.org/10.5194/acp-2022-628
Preprint. Discussion started: 23 September 2022


Atmospheric Chemistry and Physics Discussions

311 The film is eventually compressed to a limiting point where the monolayer collapses as
312 the materials leaves the 2D film (Lee, 2008). In general, the collapse is an irreversible
313 process, and the collapsed material does not reintegrate into the monolayer as the
314 surface pressure decreases.

315 Although the π-A isotherms of individual fatty acids have been well studied, the
316 phase behavior of the mixed binary and ternary systems still needs to be further
317 explored. Pure natural seawater without spreading surface-active fatty acids does not
318 cause observable changes in the surface pressure, indicating that surface-active
319 impurities are either absent or have too low concentrations to cause film formation.
320 When myristic acid spreads on the water surface, it undergoes a long liquid phase, with
321 a lower collapse pressure of ~27 mN $m^{-1}$ and area per molecule as low as 5 $Å^2$. This is
322 due to the relatively high solubility of MA molecules in the aqueous phase, resulting in
323 a large loss of molecules in the monolayer. For palmitic acid monolayer, it goes through
324 a relatively short gaseous phase and rapidly enters the liquid phase. After experiencing
325 a kink point at ~40 mN $m^{-1}$, it continues to rise to ~52 mN $m^{-1}$ and collapses. Both the
326 lift-off area and molecular area of the stearic acid film decrease. This is caused by the
327 fact that the interaction (van der Waals force) between the molecules increases as the
328 molecular weight of long chain fatty acid increases. That is, increased attraction leads
329 to a decrease in distance between molecules.

330 When fatty acids are mixed in a certain molar ratio and spread onto the interface
331 water, it is found that the π-A isotherm lies between the pure fatty acids and is closer to
332 that of stearic acid, but the mean molecular area is relatively smaller. Consequently, the

https://doi.org/10.5194/acp-2022-628
Preprint. Discussion started: 23 September 2022


Atmospheric Chemistry and Physics Discussions

longer fatty acids will dominate the lateral interactions of the SSA membrane, which makes the membrane more rigid due to the larger sum of diffusive interactions. A previous study has shown that PA and SA account for approximately two-thirds of the total saturated fatty acids in fine SSA particles, with MA being the third most abundant species (Cochran et al., 2016). In view of the true proportion of fatty acids in the nascent sea spray particles, we used a ternary fatty acid membrane proxy system composed of MA, PA, and SA (2:4:3 molar ratio) in the following experiments involving Langmuir isotherms.

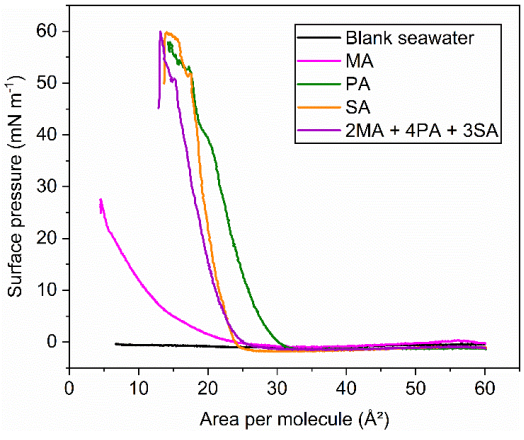


Figure 3. π-A isotherms of myristic acid, palmitic acid, stearic acid and mixed fatty acids. The black trace represents the background natural seawater solution with no fatty acid spread.

### 3.3 Effect of soluble saccharides on the phase behavior of mixed monolayers

An effective way to test whether soluble saccharides associate with lipid membranes is to examine the effect of these saccharides on the phase behavior of lipid films. The π-A isotherm provides us with rich information about the stability or fluidity of the

https://doi.org/10.5194/acp-2022-628
Preprint. Discussion started: 23 September 2022


Atmospheric Chemistry and Physics Discussions

monolayer and molecular area under membrane compression (Nakata et al., 2012). Both glucose and trehalose are highly soluble (>1.0 g $L^{-1}$) in water. However, this solubility does not preclude their presence on the surface. According to some previous studies, the dissolved organic carbon concentration is about 0.7–1.0 mg carbon $L^{-1}$ (Quinn et al., 2015; Hasenecz et al., 2019). Considering that saccharides in the ocean represent approximately 20% of the dissolved organic carbon, the saccharide concentration is about 0.14–0.20 mg $L^{-1}$ (De Vasquez et al., 2022). The Glucose and Trehalose concentrations used for the π-A isotherms are approximately 3–4 orders of magnitude greater than the saccharide concentration in dissolved organic matter, maintaining detectivity within the π-A isotherms. Furthermore, high concentrations used here are still relevant, considering the evaporation process in aged sea spray aerosols (Hasenecz et al., 2020).

Figure 4 shows the π-A isotherms of mixed fatty acids on natural seawater subphases containing different concentrations (varied between 0.1 and 5.0 g $L^{-1}$) of glucose or trehalose. In this case, the surface pressure of the fatty acid monolayer is equal to that of the fatty acid monolayer with the addition of saccharides, provided that the saccharide molecules do not affect the monolayer. At a low concentration of 0.1 g $L^{-1}$, both saccharides had little overall effect on the phase behavior of fatty acid monolayers. However, they resulted in a smaller lift-off area for the monolayer compared to pure natural seawater. As the Glucose and Trehalose subphase concentration increases, the monolayers are expanded, taking up a larger mean molecular area, which is consistent with previous research (Crowe et al., 1984). This noticeable expansion can be observed

https://doi.org/10.5194/acp-2022-628
Preprint. Discussion started: 23 September 2022


Atmospheric Chemistry and Physics Discussions

371 from the lift-off to collapse, indicating that saccharides participate in and disrupt the
372 monolayer structure. This increase may result from Glucose and Trehalose displacing
373 a significant amount of surface water surrounding the lipid headgroups and integrating
374 into the mixed monolayer by forming hydrogen bonds, which leads to an increase in
375 the lateral area of the fatty acid molecules (Roy et al., 2016). Spectral evidence is
376 needed to further clarify whether intercalation occurs. Based on the results from π-A
377 isotherms, we conclude that the spacing of fatty acids in the monolayer by saccharides
378 also increases the fluidity of the membrane.

379 More surprisingly, we observed that the isotherms of the two saccharide matrices do
380 not exhibit much difference at the concentrations of 0.5 g $L^{-1}$ and 1.0 g $L^{-1}$. When the
381 saccharide concentration keeps increasing to 5.0 g $L^{-1}$, the molecular packing density
382 on the interface decreases, and the apparent molecular area increases. In the presence
383 of glucose and trehalose, the lift-off areas increased by 9 and 10 $Å^2$, respectively. Thus,
384 it is effectively demonstrated that the more soluble saccharide molecules are added, the
385 more fatty acid molecules joined to more saccharides or more sites per saccharide
386 molecule remain separated. Another distinguishing feature of the fatty acid isotherms
387 is the change of slope above ~40 mN $m^{-1}$. This result could be interpreted as the
388 saccharide being "squeezed" out of the insoluble film, resulting in higher monolayer
389 compressibility. By squeezing saccharide molecules out of the monolayer, the isotherms
390 at high surface pressure behave similarly to other isotherms with low saccharide
391 concentrations. The difference is that with the increase of structural complexity of
392 saccharide, the effect of Trehalose at the same concentration is more prominent. The α,

https://doi.org/10.5194/acp-2022-628
Preprint. Discussion started: 23 September 2022


Atmospheric Chemistry and Physics Discussions

393 α, 1,1-linkage between two glucose subunits in trehalose is considered to provide an
394 elastic and rigid balance, thus allowing for strong interactions with multiple fatty acid
395 headgroups (Clark et al., 2015). The expansion effect promoted by soluble saccharides
396 is more relevant at lower surface pressure when alkyl chains are farther apart from each
397 other.

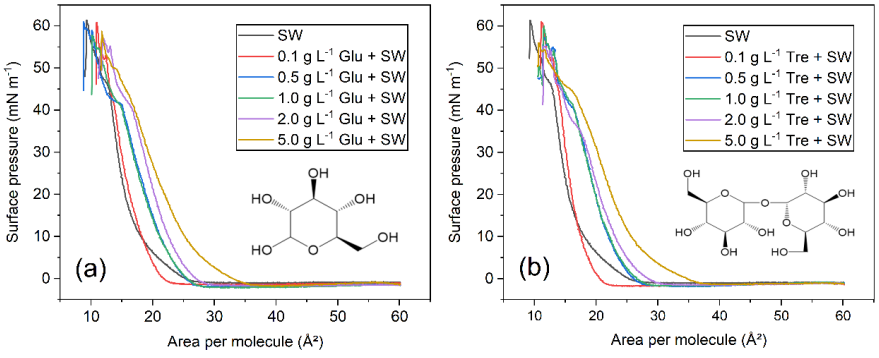


398

399 Figure 4. π-A isotherms of mixed fatty acids in the SW subphase with several
400 concentration gradients of (a) glucose, and (b) trehalose. The inset shows the molecular
401 structures of glucose and trehalose.

402 The existence of such expansion behavior in the presence of saccharides implies a
403 degree of complexity and heterogeneous distribution of species in the interfacial region.
404 In addition, trehalose exhibits more affinity for fatty acids in the monolayer than
405 glucose, in part because trehalose interacts less with neighboring saccharide molecules
406 (Leekumjorn and Sum, 2008). These results suggest that trehalose tends to bind to
407 monolayer surfaces better than glucose, forming a subsurface. This difference can be
408 explained by the fact that glucose is smaller than trehalose and has greater mobility in
409 combination with other glucose molecules. As a result, trehalose binds more readily to
410 lipid monolayer surfaces than glucose and is less mobile, as is evident from

https://doi.org/10.5194/acp-2022-628
Preprint. Discussion started: 23 September 2022


Atmospheric Chemistry and Physics Discussions

411 experimental observations. This is consistent with the result of Crowe et al. on the effect
412 of saccharides (glucose, sucrose, trehalose and raffinose) on the properties of 1,2-
413 dimyristoyl-*sn*-glycero-3-phosphocholine (DMPC) and 1,2-dipalmitoyl-*sn*-glycero-3-
414 phosphocholine (DPPC) monolayers. That is, the area per lipid increases with the
415 increase of saccharide concentration, and trehalose provides the largest lateral
416 monolayer expansion (Crowe et al., 1984). Clarifying and refining the interaction
417 mechanisms by which lipid molecules interact with saccharides is critical to any attempt
418 to model such chemical phenomena occurring at environmentally relevant interfaces.

419 **3.4 Effect of soluble saccharides on the interfacial structure of mixed monolayers**

420 PM-IRRAS is a surface sensitive technique that allows further study of the possible
421 effects of soluble saccharides on lipid interfacial organization at the molecular level.
422 Figure 5 shows the IRRAS spectra for mixed fatty acid monolayers at two different
423 saccharides containing subphases at a surface pressure of ~30 mN $m^{-1}$. This phase
424 corresponds to the two-dimensional LC phase. Figure S3 shows the IRRAS spectra of
425 mixed fatty acids measured at different surface pressures. It can be observed that with
426 the increase of surface pressure, the intensity of the peaks also increases accordingly,
427 reaching a relatively stable level around 30 mN $m^{-1}$. Considering the stability of the
428 monolayer, this surface pressure was chosen to obtain the desired infrared spectra.

429 The absorption band in the 3000–2800 $cm^{-1}$ region shown in Figure 5 is ascribed to
430 the CH stretching vibration of the alkyl chain. The main features at ~2916 and ~2850
431 $cm^{-1}$ are related to antisymmetric ($\nu_{as}(CH_2)$) and symmetric ($\nu_s(CH_2)$) stretching modes

https://doi.org/10.5194/acp-2022-628
Preprint. Discussion started: 23 September 2022


Atmospheric Chemistry and Physics Discussions

of methylene of mixed fatty acids, respectively. The $\nu_{as}(CH_2)$ feature consistently remains stronger than $\nu_s(CH_2)$ with the increase of Glucose and Trehalose concentrations. These two band positions are often used to be empirically correlated with the order and organization within the alkyl monolayer adsorbed to the water interface, with higher wavenumbers corresponding to disordered *gauche* conformers. Conversely, low wavenumbers indicate that the alkyl chain of lipids is well ordered with preferential *all-trans* characteristics. In this work, the relatively low frequencies of $\nu_{as}(CH_2)$ (2916 $cm^{-1}$) and $\nu_s(CH_2)$ (2850 $cm^{-1}$) hint that the molecular conformation of the fatty acid alkyl chains is dominated by the highly ordered *all-trans* conformation (Li et al., 2019). Despite the concentration range of saccharides varied widely, the positions of $\nu_{as}(CH_2)$ and $\nu_s(CH_2)$ showed modest sensitivity to shift, suggesting very minor changes in the conformation of the alkyl chain. The relative weak antisymmetric ($\nu_{as}(CH_3)$) and symmetric methyl stretching ($\nu_s(CH_3)$) vibrations were observed at ~2958 and ~2877 $cm^{-1}$, respectively. These results indicate that the penetration of soluble saccharides is only superficial (along the lipid surface) and has little effect on the alkyl tail arrangement. Therefore, it is further deduced that the stabilization mechanism between saccharides and fatty acid molecules may occur in the headgroup region.

https://doi.org/10.5194/acp-2022-628
Preprint. Discussion started: 23 September 2022


Atmospheric Chemistry and Physics Discussions

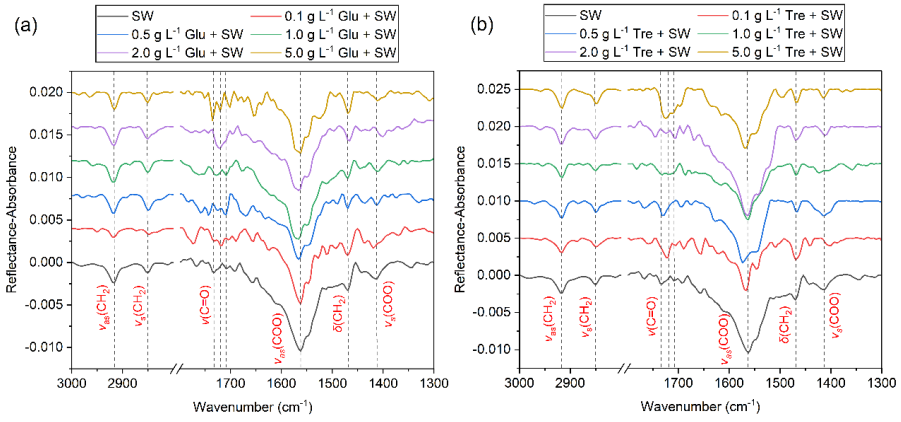


Figure 5. PM-IRRAS spectra of mixed fatty acids at the air/seawater interface at different (a) glucose, and (b) trehalose concentration in the subphase.

Carboxylic acids possess one hydrogen bond donor (hydroxyl) and one hydrogen bond acceptor (carbonyl) within the same functional group, the carboxyl group. The carbonyl stretch mode ($\nu$(C=O)) of the carboxyl group at ~1732 $cm^{-1}$ (unhydrogen bonded) was observed in seawater. This band component is put down to the conformation with the carbonyl group almost parallel to the water surface. In the presence of saccharides, the unhydrated C=O band was observed to be depressed, and the singly and doubly hydrogen bonded carbonyl components at ~1720 and ~1708 $cm^{-1}$ became dominant (Johann et al., 2001). The presence of hydrogen bonds between saccharides and the carbonyls of fatty acids is well correlated with the observed shifts in the infrared absorption band of carbonyl groups. Using FTIR experiments, Luzardo et al. (2000) showed that trehalose shifts the vibrational frequency of the carbonyl group to a lower value, which is an evidence of the existence of direct hydrogen bonding between trehalose and lipid carbonyl groups. We believe that saccharides displace water surrounding the fatty acid polar headgroups and interact strongly with both water and

https://doi.org/10.5194/acp-2022-628
Preprint. Discussion started: 23 September 2022


Atmospheric Chemistry and Physics Discussions

lipid headgroups, resulting in a slight increase in hydration near the monolayer interface.

The nonmonotonic hydrogen bond strength shows that the interaction at the interface manifests as competing contributions that dominate at different concentrations. Within the concentration range studied, saccharides tend to "displace" water, creating unique environments. In some recent studies, this "water displacement" hypothesis was supported by molecular dynamics (MD) simulations, fluorescence microscopy and nuclear magnetic resonance (NMR) (Lambruschini et al., 2000; You et al., 2021; Kapla et al., 2015). Previous MD simulation studies showed that the hydrogen bond lifetime between trehalose and membrane was longer than that established between water and membrane (Villarreal et al., 2004). This is because water molecules are more mobile and can exchange more frequently at the interface than trehalose. Another study also confirmed that sugar-lipid hydrogen bonds are stronger than water-lipid hydrogen bonds due to low endothermicity and they remain largely intact even at very high sugar concentrations (You et al., 2021).

Long chain fatty acid amphiphiles that spread as a monolayer on the alkaline subphase undergo dissociation. The ratio of neutral fatty acids and ionized carboxylates in the monolayer depends on the pH of the subphase solution. At natural oceanic conditions (pH~8.0), deprotonation of the carboxylic acid groups results in two carboxylate stretches. The broad and strong antisymmetric carboxylate stretch ($\nu_{as}$(COO)) were observed at ~1562 $cm^{-1}$, and the symmetric carboxylate stretch ($\nu_{s}$(COO)) at ~1412 $cm^{-1}$. The presence of salt in seawater caused the $\nu_{as}$(COO) to split into three peaks at ~1562, ~1547 and ~1524 $cm^{-1}$. A distinctive feature in all spectra

https://doi.org/10.5194/acp-2022-628
Preprint. Discussion started: 23 September 2022


Atmospheric Chemistry and Physics Discussions

obtained at ~1469 $cm^{-1}$ was assigned to the $CH_2$ scissoring vibration ($\delta(CH_2)$) of the aliphatic chain (Muro et al., 2010). This wavenumber value somewhat indicates an orthorhombic subcell structure. It should be noted that the $\delta(CH_2)$ vibrational position for the surface membrane of the mixed fatty acids reported here is relatively insensitive to saccharides and their concentrations. This observation confirms the conclusions drawn from the $\nu_{as}(CH_2)$ and $\nu_s(CH_2)$ wavenumbers that higher alkyl chain conformational orders are obtained either on the surface of pure seawater or on subphases containing Glucose or Trehalose.

### 3.5 Effect of soluble saccharides on particle morphology

Particle morphology can affect the surface composition, heterogeneous chemistry, gas-particle partitioning of semi-volatile organics and water uptake of aerosols (Unger et al., 2020; Ruehl et al., 2016; Lee et al., 2021). We examined the particle morphology and qualitatively compared SSAs between different model systems, including the mixed effects of saccharides and fatty acids. Compared to the study by Unger et al. (2020), the samples we investigated had compositions that were closely connected to the chemical composition of sea spray aerosols.

https://doi.org/10.5194/acp-2022-628
Preprint. Discussion started: 23 September 2022


Atmospheric Chemistry and Physics Discussions

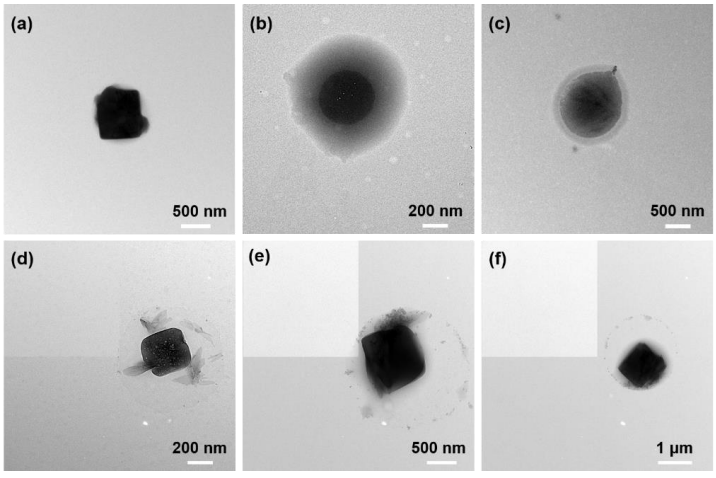


Figure 6. TEM images of morphology identified for sea spray aerosols produced from (a) natural seawater, (b) seawater with glucose and (c) seawater with trehalose without fatty acids organic layer; (d) natural seawater with fatty acids, (e) seawater with glucose and fatty acids, (f) seawater with trehalose and fatty acids.

Figure 6 depicts TEM images of SSA particles generated by plunging jet sea spray aerosol generator, which can provide clues about how saccharide and/or fatty acid components are interacting with sea salt. As can be seen from the Figure 6a, SSA produced from pure natural seawater by plunging jet exhibited a prism-like morphology that is predominantly inorganic in nature (Lee et al., 2020). This standard cubic shape also suggests that NaCl is an important component of natural seawater sample used in this study. The morphology of SSA particles was strongly affected by the incorporation of saccharides. In the presence of saccharides, the images indicate that these SSA particles exhibit a core-shell morphology with the shell portion being mainly organic in composition, whereas sea salt core are more spherical in nature, demonstrating that organic substances inhibit the cubic crystallization of NaCl. The core-shell

https://doi.org/10.5194/acp-2022-628
Preprint. Discussion started: 23 September 2022


Atmospheric Chemistry and Physics Discussions

morphologies adopted here are congruent with previous studies on the NaCl/Glucose binary system and authentic SSA samples observed using atomic force microscopy (Ray et al., 2019; Estillore et al., 2017).

The particles in Figures 6b–c existing as mixtures of salt and organic matter are also commonly labeled as sea salt-organic carbon (SS-OC) (Ault et al., 2013a). The core-shell morphology was found to be highly dependent on the salt-to-organic ratio and varied with the nature and solubility of organic components (Estillore et al., 2017). For example, previous studies have showed that adding organic material to aqueous solution, particle morphology, crystallization behavior and optical properties were changed as the amount of organic content in the particles increased (Ault et al., 2013b; Freedman et al., 2009). Furthermore, the shell thickness of core-shell SSA shows size-dependent variability. Specifically, larger core-shell particles generally displayed relatively thinner coatings, while smaller core-shell particles displayed thicker coatings. However, as shown in Figures 6d–f, the presence of fatty acid layer on the surface not only has little effect on the morphology of SSA particles, but also weakens the morphology modification of SSA particles by saccharides. In a word, the results presented in this study suggest that the heterogeneity within a particle type is a function of seawater chemistry.

### 3.6 Proposed mechanism for bulk saccharide transfer to SSA

The molecular level interactions between small saccharides and fatty acids discussed in previous sections can be summarized using the model presented in Figure 7. Aqueous

https://doi.org/10.5194/acp-2022-628
Preprint. Discussion started: 23 September 2022


Atmospheric Chemistry and Physics Discussions

542 aerosols coated by surface-active organic matter (Figure 7a), such as SSA, generally
543 hold inverse micelle structures with hydrophilic headgroups pointing toward the
544 aqueous phase and hydrophobic tails pointing toward the gas phase (Blackshaw et al.,
545 2019). At the center of the inverse micelle, a water pool is formed that can dissolve
546 polar substances such as saccharides, proteins, enzymes, amino acids and nucleic acid.
547 This unique physicochemical environment may enhance the possibility of saccharides
548 transfer to SSA. Through the Langmuir surface pressure-area experiment combined
549 with infrared reflection-absorption spectroscopy, we initially explored the possible
550 mechanism of the transfer of saccharides at the air/water interface. In a nutshell, we
551 infer that saccharides initially in the aqueous phase move steadily to the interface and
552 act as a substituent for water molecules, and locate in the headgroup region of the fatty
553 acids. During the binding process, the saccharides displace the oriented water molecules
554 that are bound to the fatty acids through hydrogen bonds, establishing new hydrogen
555 bonds with the carbonyl group of fatty acids (You et al., 2021).

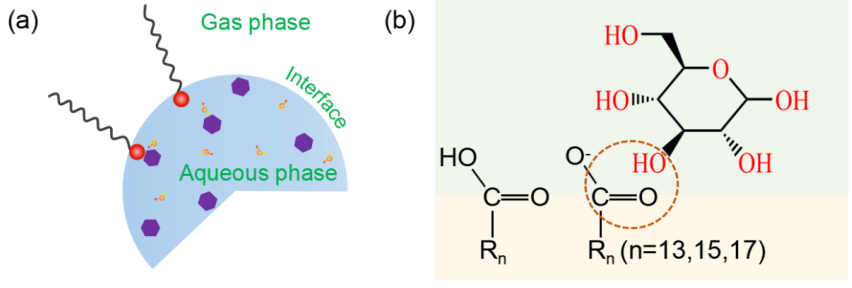


556

557 Figure 7. (a) Proposed model of fatty acid-saccharide interaction at the air/water
558 interface. (b) Description of possible mechanisms of fatty acid-saccharide interaction
559 at the air/water interface.

https://doi.org/10.5194/acp-2022-628
Preprint. Discussion started: 23 September 2022


Atmospheric Chemistry and Physics Discussions

### 3.7 Atmospheric implications

Despite extensive efforts, the exhaustive relationships between ocean organic carbon pools and the chemical composition of SSAs are still outstanding. The coupling of this sea spray aerosol simulation generator with the interfacial monolayer model lays the foundation for further studies of the material relationship between the ocean and SSA. The research reported here yielded two key findings. First, the SSA production and particle size distribution are usually extremely sensitive to organic matter, and small saccharides dissolved in seawater are critical to the formation, size and composition of SSA. Our results strongly support that saccharides can greatly promote the generation of SSA particles and make SSA show core-shell morphology characteristics. A previous study revealed that the SSA number concentration in coastal samples was inversely correlated with salinity, with several organic tracers, including dissolved and chromophoric organic carbon (DOC, CDOM), marine microgels, and chlorophyll a (Chl-a) being positively correlated, but not associated with viral and bacterial abundances (Park et al., 2019). Therefore, the factors that affect the emission of SSA have not been fully clarified. Other limitations to this study include the poor representation, by the simple chemical structural models, of the myriad complex biomolecules that exist in the ocean, spanning dissolved, colloidal and particulate matter. It is recommended that future studies targeting the production and property of SSA include the effects of different types of organic matter to determine whether they fully mimic the arrays of SSA particles, and include more complete organic matter systems as well as biological species.

https://doi.org/10.5194/acp-2022-628
Preprint. Discussion started: 23 September 2022


Atmospheric Chemistry and Physics Discussions

582 Second, it has been suggested that the abundant organic content in SSA plays a key
583 role in determining the cloud condensation nucleation and ice nucleating activity
584 (O'dowd et al., 2004). Therefore, climate models demand a predictive representation of
585 SSA chemical composition to accurately simulate climate processes in the marine
586 boundary layer (Burrows et al., 2016; Bertram et al., 2018). However, the source of
587 organic enrichment observed in SSA remains speculative, which poses challenges to
588 the modeling of the aerosol impact on atmospheric chemistry and climate science. A
589 recent study has raised that the cooperative adsorption of saccharides with insoluble
590 lipid monolayers may make important contributions to the sea spray aerosols and even
591 have climatic consequences with broad research prospects (Burrows et al., 2014). In
592 this work, we used the Langmuir monolayer to model possible interactions between
593 subphase soluble saccharides and surface fatty acid molecules. A subsequent study used
594 infrared reflection-absorption spectroscopy to determine the interaction mechanism
595 between two simple soluble saccharides and tightly packed fatty acids monolayers at
596 the air/water interface. Combining the above experimental data, we infer that a
597 hydrogen bond network between saccharides and the carbonyl group of surface
598 insoluble fatty acid molecules contributes to its transfer from the ocean to the
599 atmosphere. At present, this mechanism of saccharide transfer and enrichment has not
600 been emphasized in the model describing SSA formation. To further examine the
601 feasibility of the hydrogen bonding mechanism as an interfacial organic enrichment
602 mechanism, it is necessary to further explore and verify the interaction of other
603 carbohydrates with common surface-insoluble molecules in future studies.

https://doi.org/10.5194/acp-2022-628
Preprint. Discussion started: 23 September 2022


Atmospheric Chemistry and Physics Discussions

## 4 Conclusions

In summary, we simulated the production of SSA in natural seawater spiked with two common soluble saccharides using a plunging water jet generator and revealed the possible mechanism of saccharide transfer from bulk seawater into SSA combined with surface sensitive infrared spectroscopy techniques. We confirmed that glucose and trehalose can significantly promote the production of SSA and alter the surface morphology of SSA particles. This highlights the potential for a direct oceanic source of carbohydrate organics through bubble bursting. In addition, trehalose showed stronger promoting ability than glucose, while the surface fatty acid layer played an inhibitory role. Using the mixture of saturated fatty acids MA, PA and SA as the proxy of SSA surface film, the π-A isotherms provided strong evidence that saccharides can interact with insoluble fatty acid monolayers and be absorbed at the monolayer, which caused expansion of the monolayer and made the films heterogeneous. According to the IRRAS spectra, soluble saccharides did not produce an observable effect on the order of fatty acid alkyl chains. We further infer that soluble saccharides are mainly located on the subsurface below the monolayer, and interact with carbonyl groups of fatty acids by forming hydrogen bonds to facilitate their sea-air transfer. Crucially, this work provides physical and molecular signatures of potentially important saccharides transfer mechanism with general implications for understanding how saccharide-lipid-water interactions affect sea spray aerosol systems.

https://doi.org/10.5194/acp-2022-628
Preprint. Discussion started: 23 September 2022


Atmospheric Chemistry and Physics Discussions

## Data availability

Data are available by contacting the corresponding author.

## Supplement

The supplement related to this article is available online at:

## Author contributions

MX: conceived the experiment, data curation, formal analysis, writing original draft, writing-review & editing. NTT: writing - review & editing. JL: writing - review & editing. LD: supervision, conceived the experiment, funding acquisition, writing - review & editing.

## Competing interests

The author declare that they have no conflict of interest.

## Financial support

The authors acknowledge support from National Natural Science Foundation of China (22076099, 21876098), the Department of Education of Shandong Province (2019KJD007), and Fundamental Research Fund of Shandong University (2020QNQT012).

https://doi.org/10.5194/acp-2022-628
Preprint. Discussion started: 23 September 2022


Atmospheric Chemistry and Physics Discussions

## References

Ault, A. P., Guasco, T. L., Ryder, O. S., Baltrusaitis, J., Cuadra-Rodriguez, L. A., Collins, D. B., Ruppel, M. J., Bertram, T. H., Prather, K. A., and Grassian, V. H.: Inside versus outside: Ion redistribution in nitric acid reacted sea spray aerosol particles as determined by single particle analysis, J. Am. Chem. Soc., 135, 14528-14531, 10.1021/ja407117x, 2013a.

Ault, A. P., Moffet, R. C., Baltrusaitis, J., Collins, D. B., Ruppel, M. J., Cuadra-Rodriguez, L. A., Zhao, D. F., Guasco, T. L., Ebben, C. J., Geiger, F. M., Bertram, T. H., Prather, K. A., and Grassian, V. H.: Size-dependent changes in sea spray aerosol composition and properties with different seawater conditions, Environ. Sci. Technol., 47, 5603-5612, 10.1021/es400416g, 2013b.

Bertram, T. H., Cochran, R. E., Grassian, V. H., and Stone, E. A.: Sea spray aerosol chemical composition: Elemental and molecular mimics for laboratory studies of heterogeneous and multiphase reactions, Chem. Soc. Rev., 47, 2374-2400, 10.1039/c7cs00008a, 2018.

Blackshaw, K. J., Varmecky, M. G., and Patterson, J. D.: Interfacial structure and partitioning of nitrate ions in reverse micelles, J. Phys. Chem. A, 123, 336-342, 10.1021/acs.jpca.8b09751, 2019.

Burrows, S. M., Ogunro, O., Frossard, A. A., Russell, L. M., Rasch, P. J., and Elliott, S. M.: A physically based framework for modeling the organic fractionation of sea spray aerosol from bubble film Langmuir equilibria, Atmos. Chem. Phys., 14, 13601-13629, 10.5194/acp-14-13601-2014, 2014.

Burrows, S. M., Gobrogge, E., Fu, L., Link, K., Elliott, S. M., Wang, H. F., and Walker, R.: OCEANFILMS-2: Representing coadsorption of saccharides in marine films and potential impacts on modeled marine aerosol chemistry, Geophys. Res. Lett., 43, 8306-8313, 10.1002/2016gl069070, 2016.

Christiansen, S., Salter, M. E., Gorokhova, E., Nguyen, Q. T., and Bilde, M.: Sea spray aerosol formation: Laboratory results on the role of air entrainment, water temperature and phytoplankton biomass, Environ. Sci. Technol., 53, 13107-13116, 10.1021/acs.est.9b04078, 2019.

Clark, G. A., Henderson, J. M., Heffern, C., Akgun, B., Majewski, J., and Lee, K. Y. C.: Synergistic interactions of sugars/polyols and monovalent salts with phospholipids depend upon sugar/polyol complexity and anion identity, Langmuir, 31, 12688-12698, 10.1021/acs.langmuir.5b02815, 2015.

Cochran, R. E., Laskina, O., Jayarathne, T., Laskin, A., Laskin, J., Lin, P., Sultana, C., Lee, C., Moore, K. A., Cappa, C. D., Bertram, T. H., Prather, K. A., Grassian, V. H., and Stone, E. A.: Analysis of organic anionic surfactants in fine and coarse fractions of freshly emitted sea spray aerosol, Environ. Sci. Technol., 50, 2477-2486, 10.1021/acs.est.5b04053, 2016.

Cochran, R. E., Laskina, O., Trueblood, J. V., Estillore, A. D., Morris, H. S., Jayarathne, T., Sultana, C. M., Lee, C., Lin, P., Laskin, J., Laskin, A., Dowling, J. A., Qin, Z., Cappa, C. D., Bertram, T. H., Tivanski, A. V., Stone, E. A., Prather, K. A., and Grassian, V. H.:

https://doi.org/10.5194/acp-2022-628
Preprint. Discussion started: 23 September 2022




683 Molecular diversity of sea spray aerosol particles: Impact of ocean biology on particle
684 composition and hygroscopicity, Chem, 2, 655-667, 10.1016/j.chempr.2017.03.007,
685 2017.
686 Collins, D. B., Zhao, D. F., Ruppel, M. J., Laskina, O., Grandquist, J. R., Modini, R. L.,
687 Stokes, M. D., Russell, L. M., Bertram, T. H., Grassian, V. H., Deane, G. B., and Prather,
688 K. A.: Direct aerosol chemical composition measurements to evaluate the
689 physicochemical differences between controlled sea spray aerosol generation schemes,
690 Atmos. Meas. Tech., 7, 3667-3683, 10.5194/amt-7-3667-2014, 2014.
691 Cravigan, L. T., Mallet, M. D., Vaattovaara, P., Harvey, M. J., Law, C. S., Modini, R.
692 L., Russell, L. M., Stelcer, E., Cohen, D. D., Olsen, G., Safi, K., Burrell, T. J., and
693 Ristovski, Z.: Sea spray aerosol organic enrichment, water uptake and surface tension
694 effects, Atmos. Chem. Phys., 20, 7955-7977, 10.5194/acp-20-7955-2020, 2020.
695 Crocker, D. R., Deane, G. B., Cao, R. C., Santander, M. V., Morris, C. K., Mitts, B. A.,
696 Dinasquet, J., Amiri, S., Malfatti, F., Prather, K. A., and Thiemens, M. H.: Biologically
697 induced changes in the partitioning of submicron particulates between bulk seawater
698 and the sea surface microlayer, Geophys. Res. Lett., 49, e2021GL094587,
699 10.1029/2021GL094587, 2022.
700 Crowe, J. H., Whittam, M. A., Chapman, D., and Crowe, L. M.: Interactions of
701 phospholipid monolayers with carbohydrates, Biochim. Biophys. Acta, Biomembr.,
702 769, 151-159, 10.1016/0005-2736(84)90018-x, 1984.
703 Cunliffe, M., Engel, A., Frka, S., Gašparović, B., Guitart, C., Murrell, J. C., Salter, M.,
704 Stolle, C., Upstill-Goddard, R., and Wurl, O.: Sea surface microlayers: A unified
705 physicochemical and biological perspective of the air–ocean interface, Prog. Oceanogr.,
706 109, 104-116, 10.1016/j.pocean.2012.08.004, 2013.
707 de Vasquez, M. G. V., Rogers, M. M., Carter-Fenk, K. A., and Allen, H. C.: Discerning
708 poly- and monosaccharide enrichment mechanisms: Alginate and glucuronate
709 adsorption to a stearic acid sea surface microlayer, ACS Earth Space Chem., 6, 1581-
710 1595, 10.1021/acsearthspacechem.2c00066, 2022.
711 Elliott, S., Burrows, S. M., Deal, C., Liu, X., Long, M., Ogunro, O., Russell, L. M., and
712 Wingenter, O.: Prospects for simulating macromolecular surfactant chemistry at the
713 ocean-atmosphere boundary, Environ. Res. Lett., 9, 064012, 10.1088/1748-
714 9326/9/6/064012, 2014.
715 Estillore, A. D., Morris, H. S., Or, V. W., Lee, H. D., Alves, M. R., Marciano, M. A.,
716 Laskina, O., Qin, Z., Tivanski, A. V., and Grassian, V. H.: Linking hygroscopicity and
717 the surface microstructure of model inorganic salts, simple and complex carbohydrates,
718 and authentic sea spray aerosol particles, Phys. Chem. Chem. Phys., 19, 21101-21111,
719 10.1039/c7cp04051b, 2017.
720 Freedman, M. A., Hasenkopf, C. A., Beaver, M. R., and Tolbert, M. A.: Optical
721 properties of internally mixed aerosol particles composed of dicarboxylic acids and
722 ammonium sulfate, J. Phys. Chem. A, 113, 13584-13592, 10.1021/jp906240y, 2009.
723 Frossard, A. A., Russell, L. M., Burrows, S. M., Elliott, S. M., Bates, T. S., and Quinn,
724 P. K.: Sources and composition of submicron organic mass in marine aerosol particles,
725 J. Geophys. Res.-Atmos., 119, 12977-13003, 10.1002/2014jd021913, 2014.
726 Hasenecz, E. S., Kaluarachchi, C. P., Lee, H. D., Tivanski, A. V., and Stone, E. A.:

https://doi.org/10.5194/acp-2022-628
Preprint. Discussion started: 23 September 2022




727 Saccharide transfer to sea spray aerosol enhanced by surface activity, calcium, and
728 protein interactions, ACS Earth Space Chem., 3, 2539-2548,
729 10.1021/acsearthspacechem.9b00197, 2019.
730 Hasenecz, E. S., Jayarathne, T., Pendergraft, M. A., Santander, M. V., Mayer, K. J.,
731 Sauer, J., Lee, C., Gibson, W. S., Kruse, S. M., Malfatti, F., Prather, K. A., and Stone,
732 E. A.: Marine bacteria affect saccharide enrichment in sea spray aerosol during a
733 phytoplankton bloom, ACS Earth Space Chem., 4, 1638-1649,
734 10.1021/acsearthspacechem.0c00167, 2020.
735 Hawkins, L. N. and Russell, L.: Polysaccharides, proteins, and phytoplankton
736 fragments: Four chemically distinct types of marine primary organic aerosol classified
737 by single particle spectromicroscopy, Adv. Meteorol., 2010, 612132,
738 10.1155/2010/612132, 2010.
739 Hultin, K. A. H., Nilsson, E. D., Krejci, R., Martensson, E. M., Ehn, M., Hagstrom, A.,
740 and de Leeuw, G.: In situ laboratory sea spray production during the Marine Aerosol
741 Production 2006 cruise on the northeastern Atlantic Ocean, J. Geophys. Res.-Atmos.,
742 115, D06201, 10.1029/2009jd012522, 2010.
743 Jaegle, L., Quinn, P. K., Bates, T. S., Alexander, B., and Lin, J. T.: Global distribution
744 of sea salt aerosols: new constraints from in situ and remote sensing observations,
745 Atmos. Chem. Phys., 11, 3137-3157, 10.5194/acp-11-3137-2011, 2011.
746 Johann, R., Vollhardt, D., and Mohwald, H.: Study of the pH dependence of head group
747 bonding in arachidic acid monolayers by polarization modulation infrared reflection
748 absorption spectroscopy, Colloid Surf. A-Physicochem. Eng. Asp., 182, 311-320,
749 10.1016/s0927-7757(00)00812-8, 2001.
750 Kapla, J., Engstrom, O., Stevensson, B., Wohlert, J., Widmalm, G., and Maliniak, A.:
751 Molecular dynamics simulations and NMR spectroscopy studies of trehalose-lipid
752 bilayer systems, Phys. Chem. Chem. Phys., 17, 22438-22447, 10.1039/c5cp02472b,
753 2015.
754 King, S. M., Butcher, A. C., Rosenoern, T., Coz, E., Lieke, K. I., de Leeuw, G., Nilsson,
755 E. D., and Bilde, M.: Investigating primary marine aerosol properties: CCN activity of
756 sea salt and mixed inorganic-organic particles, Environ. Sci. Technol., 46, 10405-10412,
757 10.1021/es300574u, 2012.
758 Lambruschini, C., Relini, A., Ridi, A., Cordone, L., and Gliozzi, A.: Trehalose interacts
759 with phospholipid polar heads in Langmuir monolayers, Langmuir, 16, 5467-5470,
760 10.1021/la991641e, 2000.
761 Lee, C., Dommer, A. C., Schiffer, J. M., Amaro, R. E., Grassian, V. H., and Prather, K.
762 A.: Cation-driven lipopolysaccharide morphological changes impact heterogeneous
763 reactions of nitric acid with sea spray aerosol particles, J. Phys. Chem. Lett., 12, 5023-
764 5029, 10.1021/acs.jpclett.1c00810, 2021.
765 Lee, H. D., Wigley, S., Lee, C., Or, V. W., Hasenecz, E. S., Stone, E. A., Grassian, V.
766 H., Prather, K. A., and Tivanski, A. V.: Physicochemical mixing state of sea spray
767 aerosols: Morphologies exhibit size dependence, ACS Earth Space Chem., 4, 1604-
768 1611, 10.1021/acsearthspacechem.0c00153, 2020.
769 Lee, K. Y. C.: Collapse mechanisms of Langmuir monolayers, Annu. Rev. Phys. Chem.,
770 59, 771-791, 10.1146/annurev.physchem.58.032806.104619, 2008.

https://doi.org/10.5194/acp-2022-628
Preprint. Discussion started: 23 September 2022




771 Leekumjorn, S. and Sum, A. K.: Molecular dynamics study on the stabilization of
772 dehydrated lipid bilayers with glucose and trehalose, J. Phys. Chem. B, 112, 10732-
773 10740, 10.1021/jp8025489, 2008.
774 Li, S. Y., Jiang, X. T., Roveretto, M., George, C., Liu, L., Jiang, W., Zhang, Q. Z., Wang,
775 W. X., Ge, M. F., and Du, L.: Photochemical aging of atmospherically reactive organic
776 compounds involving brown carbon at the air-aqueous interface, Atmos. Chem. Phys.,
777 19, 9887-9902, 10.5194/acp-19-9887-2019, 2019.
778 Link, K. A., Spurzem, G. N., Tuladhar, A., Chase, Z., Wang, Z. M., Wang, H. F., and
779 Walker, R. A.: Cooperative adsorption of trehalose to DPPC monolayers at the water-
780 air interface studied with vibrational sum frequency generation, J. Phys. Chem. B, 123,
781 8931-8938, 10.1021/acs.jpcb.9b07770, 2019a.
782 Link, K. A., Spurzem, G. N., Tuladhar, A., Chase, Z., Wang, Z. M., Wang, H. F., and
783 Walker, R. A.: Organic enrichment at aqueous interfaces: Cooperative adsorption of
784 glucuronic acid to DPPC monolayers studied with vibrational sum frequency
785 generation, J. Phys. Chem. A, 123, 5621-5632, 10.1021/acs.jpca.9b02255, 2019b.
786 Liu, L. R., Du, L., Xu, L., Li, J. L., and Tsona, N. T.: Molecular size of surfactants
787 affects their degree of enrichment in the sea spray aerosol formation, Environ. Res.,
788 206, 112555, 10.1016/j.envres.2021.112555, 2022.
789 Luzardo, M. D., Amalfa, F., Nunez, A. M., Diaz, S., de Lopez, A. C. B., and Disalvo,
790 E. A.: Effect of trehalose and sucrose on the hydration and dipole potential of lipid
791 bilayers, Biophys. J., 78, 2452-2458, 10.1016/s0006-3495(00)76789-0, 2000.
792 Lv, C., Tsona, N. T., and Du, L.: Sea spray aerosol formation: Results on the role of
793 different parameters and organic concentrations from bubble bursting experiments,
794 Chemosphere, 252, 126456, 10.1016/j.chemosphere.2020.126456, 2020.
795 Muro, M., Itoh, Y., and Hasegawa, T.: A conformation and orientation model of the
796 carboxylic group of fatty acids dependent on chain length in a Langmuir monolayer
797 film studied by polarization-modulation infrared reflection absorption spectroscopy, J.
798 Phys. Chem. B, 114, 11496-11501, 10.1021/jp105862q, 2010.
799 Nakata, S., Shiota, T., Kumazawa, N., and Denda, M.: Interaction between a
800 monosaccharide and a phospholipid molecular layer, Colloid Surf. A-Physicochem.
801 Eng. Asp., 405, 14-18, 10.1016/j.colsurfa.2012.04.021, 2012.
802 O'Dowd, C. D., Facchini, M. C., Cavalli, F., Ceburnis, D., Mircea, M., Decesari, S.,
803 Fuzzi, S., Yoon, Y. J., and Putaud, J. P.: Biogenically driven organic contribution to
804 marine aerosol, Nature, 431, 676-680, 10.1038/nature02959, 2004.
805 Orellana, M. V., Matrai, P. A., Leck, C., Rauschenberg, C. D., Lee, A. M., and Coz, E.:
806 Marine microgels as a source of cloud condensation nuclei in the high Arctic, Proc. Natl.
807 Acad. Sci. U. S. A., 108, 13612-13617, 10.1073/pnas.1102457108, 2011.
808 Park, J., Dall'Osto, M., Park, K., Kim, J. H., Park, J., Park, K. T., Hwang, C. Y., Jang,
809 G. I., Gim, Y., Kang, S., Park, S., Jin, Y. K., Yum, S. S., Simo, R., and Yoon, Y. J.: Arctic
810 primary aerosol production strongly influenced by riverine organic matter, Environ. Sci.
811 Technol., 53, 8621-8630, 10.1021/acs.est.9b03399, 2019.
812 Partanen, A. I., Dunne, E. M., Bergman, T., Laakso, A., Kokkola, H., Ovadnevaite, J.,
813 Sogacheva, L., Baisnee, D., Sciare, J., Manders, A., O'Dowd, C., de Leeuw, G., and
814 Korhonen, H.: Global modelling of direct and indirect effects of sea spray aerosol using

https://doi.org/10.5194/acp-2022-628
Preprint. Discussion started: 23 September 2022




a source function encapsulating wave state, Atmos. Chem. Phys., 14, 11731-11752, 10.5194/acp-14-11731-2014, 2014.

Pavinatto, F. J., Caseli, L., Pavinatto, A., dos Santos, D. S., Nobre, T. M., Zaniquelli, M. E. D., Silva, H. S., Miranda, P. B., and de Oliveira, O. N.: Probing chitosan and phospholipid interactions using Langmuir and Langmuir-Blodgett films as cell membrane models, Langmuir, 23, 7666-7671, 10.1021/la700856a, 2007.

Perkins, R. and Vaida, V.: Phenylalanine increases membrane permeability, J. Am. Chem. Soc., 139, 14388-14391, 10.1021/jacs.7b09219, 2017.

Prather, K. A., Bertram, T. H., Grassian, V. H., Deane, G. B., Stokes, M. D., DeMott, P. J., Aluwihare, L. I., Palenik, B. P., Azam, F., Seinfeld, J. H., Moffet, R. C., Molina, M. J., Cappa, C. D., Geiger, F. M., Roberts, G. C., Russell, L. M., Ault, A. P., Baltrusaitis, J., Collins, D. B., Corrigan, C. E., Cuadra-Rodriguez, L. A., Ebben, C. J., Forestieri, S. D., Guasco, T. L., Hersey, S. P., Kim, M. J., Lambert, W. F., Modini, R. L., Mui, W., Pedler, B. E., Ruppel, M. J., Ryder, O. S., Schoepp, N. G., Sullivan, R. C., and Zhao, D. F.: Bringing the ocean into the laboratory to probe the chemical complexity of sea spray aerosol, Proc. Natl. Acad. Sci. U. S. A., 110, 7550-7555, 10.1073/pnas.1300262110, 2013.

Quinn, P. K., Collins, D. B., Grassian, V. H., Prather, K. A., and Bates, T. S.: Chemistry and related properties of freshly emitted sea spray aerosol, Chem. Rev., 115, 4383-4399, 10.1021/cr500713g, 2015.

Quinn, P. K., Bates, T. S., Schulz, K. S., Coffman, D. J., Frossard, A. A., Russell, L. M., Keene, W. C., and Kieber, D. J.: Contribution of sea surface carbon pool to organic matter enrichment in sea spray aerosol, Nat. Geosci., 7, 228-232, 10.1038/ngeo2092, 2014.

Ray, K. K., Lee, H. D., Gutierrez, M. A., Chang, F. J., and Tivanski, A. V.: Correlating 3D morphology, phase state, and viscoelastic properties of individual substrate-deposited particles, Anal. Chem., 91, 7621-7630, 10.1021/acs.analchem.9b00333, 2019.

Roy, A., Dutta, R., Kundu, N., Banik, D., and Sarkar, N.: A comparative study of the influence of sugars sucrose, trehalose, and maltose on the hydration and diffusion of DMPC lipid bilayer at complete hydration: Investigation of structural and spectroscopic aspect of lipid-sugar interaction, Langmuir, 32, 5124-5134, 10.1021/acs.langmuir.6b01115, 2016.

Ruehl, C. R., Davies, J. F., and Wilson, K. R.: An interfacial mechanism for cloud droplet formation on organic aerosols, Science, 351, 1447-1450, 10.1126/science.aad4889, 2016.

Russell, L. M., Hawkins, L. N., Frossard, A. A., Quinn, P. K., and Bates, T. S.: Carbohydrate-like composition of submicron atmospheric particles and their production from ocean bubble bursting, Proc. Natl. Acad. Sci. U. S. A., 107, 6652-6657, 10.1073/pnas.0908905107, 2010.

Schill, S., Burrows, S., Hasenecz, E., Stone, E., and Bertram, T.: The impact of divalent cations on the enrichment of soluble saccharides in primary sea spray aerosol, Atmosphere, 9, 476, 10.3390/atmos9120476, 2018.

Schmitt-Kopplin, P., Liger-Belair, G., Koch, B. P., Flerus, R., Kattner, G., Harir, M., Kanawati, B., Lucio, M., Tziotis, D., Hertkorn, N., and Gebefugi, I.: Dissolved organic

https://doi.org/10.5194/acp-2022-628
Preprint. Discussion started: 23 September 2022


Atmospheric Chemistry and Physics Discussions

matter in sea spray: a transfer study from marine surface water to aerosols, Biogeosciences, 9, 1571-1582, 10.5194/bg-9-1571-2012, 2012.
Unger, I., Saak, C. M., Salter, M., Zieger, P., Patanen, M., and Bjorneholm, O.: Influence of organic acids on the surface composition of sea spray aerosol, J. Phys. Chem. A, 124, 422-429, 10.1021/acs.jpca.9b09710, 2020.
van Pinxteren, M., Muller, C., Iinuma, Y., Stolle, C., and Herrmann, H.: Chemical characterization of dissolved organic compounds from coastal sea surface micro layers (Baltic Sea, Germany), Environ. Sci. Technol., 46, 10455-10462, 10.1021/es204492b, 2012.
van Pinxteren, M., Robinson, T. B., Zeppenfeld, S., Gong, X., Bahlmann, E., Fomba, K. W., Triesch, N., Stratmann, F., Wurl, O., Engel, A., Wex, H., and Herrmann, H.: High number concentrations of transparent exopolymer particles in ambient aerosol particles and cloud water – a case study at the tropical Atlantic Ocean, Atmos. Chem. Phys., 22, 5725-5742, 10.5194/acp-22-5725-2022, 2022.
van Pinxteren, M., Fomba, K. W., Triesch, N., Stolle, C., Wurl, O., Bahlmann, E., Gong, X. D., Voigtlander, J., Wex, H., Robinson, T. B., Barthel, S., Zeppenfeld, S., Hoffmann, E. H., Roveretto, M., Li, C. L., Grosselin, B., Daele, V., Senf, F., van Pinxteren, D., Manzi, M., Zabalegui, N., Frka, S., Gasparovic, B., Pereira, R., Li, T., Wen, L., Li, J. R., Zhu, C., Chen, H., Chen, J. M., Fiedler, B., Von Tumpling, W., Read, K. A., Punjabi, S., Lewis, A. C., Hopkins, J. R., Carpenter, L. J., Peeken, I., Rixen, T., Schulz-Bull, D., Monge, M. E., Mellouki, A., George, C., Stratmann, F., and Herrmann, H.: Marine organic matter in the remote environment of the Cape Verde islands - an introduction and overview to the MarParCloud campaign, Atmos. Chem. Phys., 20, 6921-6951, 10.5194/acp-20-6921-2020, 2020.
Villarreal, M. A., Diaz, S. B., Disalvo, E. A., and Montich, G. G.: Molecular dynamics simulation study of the interaction of trehalose with lipid membranes, Langmuir, 20, 7844-7851, 10.1021/la049485l, 2004.
Wang, X. F., Deane, G. B., Moore, K. A., Ryder, O. S., Stokes, M. D., Beall, C. M., Collins, D. B., Santander, M. V., Burrows, S. M., Sultana, C. M., and Prather, K. A.: The role of jet and film drops in controlling the mixing state of submicron sea spray aerosol particles, Proc. Natl. Acad. Sci. U. S. A., 114, 6978-6983, 10.1073/pnas.1702420114, 2017.
Wolf, M. J., Coe, A., Dove, L. A., Zawadowicz, M. A., Dooley, K., Biller, S. J., Zhang, Y., Chisholm, S. W., and Cziczo, D. J.: Investigating the heterogeneous ice nucleation of sea spray aerosols using prochlorococcus as a model source of marine organic matter, Environ. Sci. Technol., 53, 1139-1149, 10.1021/acs.est.8b05150, 2019.
Wurl, O., Ekau, W., Landing, W. M., and Zappa, C. J.: Sea surface microlayer in a changing ocean - A perspective, Elementa-Sci. Anthrop, 5, 31, 10.1525/elementa.228, 2017.
Xu, M. L., Tsona, N. T., Cheng, S. M., Li, J. L., and Du, L.: Unraveling interfacial properties of organic-coated marine aerosol with lipase incorporation, Sci. Total Environ., 782, 146893, 10.1016/j.scitotenv.2021.146893, 2021.
You, X., Lee, E., Xu, C., and Baiz, C. R.: Molecular mechanism of cell membrane protection by sugars: A study of interfacial H-Bond networks, J. Phys. Chem. Lett., 12,

https://doi.org/10.5194/acp-2022-628
Preprint. Discussion started: 23 September 2022


Atmospheric Chemistry and Physics Discussions

903 9602-9607, 10.1021/acs.jpclett.1c02451, 2021.
904 Zeppenfeld, S., van Pinxteren, M., van Pinxteren, D., Wex, H., Berdalet, E., Vaque, D.,
905 Dall'Osto, M., and Herrmann, H.: Aerosol marine primary carbohydrates and
906 atmospheric transformation in the Western Antarctic Peninsula, ACS Earth Space
907 Chem., 5, 1032-1047, 10.1021/acsearthspacechem.0c00351, 2021.

908